Signature of QCD critical point: Anomalous transverse velocity dependence of antiproton-proton ratio

Xiao-Feng Luo,[1,*] Ming Shao,[1] Cheng Li,[1] and Hong-Fang Chen[1]

[1] *University of Science and Technology of China, Hefei, Anhui 230026, China*

(Dated: February 27, 2009)

We formulate the QCD critical point focusing effect on transverse velocity (β_t) dependence of antiproton to proton ($\bar{p}/p$) ratio, which was recently proposed by Asakawa *et al.* as an experimental signature of QCD critical point in high energy heavy ion collisions (HICs). For quantitative analysis, Ultra-relativistic Quantum Molecular Dynamics (UrQMD) transport model and THERMal heavy-IoN generATOR (THERMINATOR) are applied to calculate the corresponding β_t dependence of $\bar{p}/p$ ratio for three gedanken focused isentropic trajectories with different focusing degree on QCD phase diagram. Finally, we obtained an observable anomaly in β_t dependence of $\bar{p}/p$ ratio, which can be employed as a signature of QCD critical point.

PACS numbers: 25.75.Ld, 24.10.Jv, 24.10.Lx, 25.70.Pq

I. INTRODUCTION

In recent years, ultra-relativistic high energy heavy ion collisions (HICs) experiments, such as SPS/CERN ($\sqrt{s_{\rm NN}} \sim 10A$ GeV) and RHIC/BNL ($\sqrt{s_{\rm NN}} \sim 200A$ GeV), have been aimed to search for the new form of matter, which is composed of deconfinement free quarks and gluons, and thus called Quark Gluon Plasma (QGP) [1, 2, 3, 4]. Lattice-QCD calculation predicts that the phase transition between hadronic and QGP phases at vanishing baryon chemical potential μ_B is crossover transition whereas at higher μ_B the transition may become first-order [5, 6]. However, there are many uncertainties for Lattice-QCD or model calculation to determine the first-order phase transition boundary as well as the location of corresponding end point, the so-called QCD Critical Point (QCP) [7]. Thus, the location and even the existence of the QCP are still open questions. The uncertainty of theoretical calculation drives us to explore the properties of hot QCD matter at higher net baryon density and find experimental evidence of the QCP. Recently, several experimental programs have planed to search for the QCP, such as the energy scan program of RHIC/BNL ($\sqrt{s_{\rm NN}} = 5 \sim 39A$ GeV) [8, 9, 10], the light ion program of NA61 experiment at SPS/CERN ($\sqrt{s_{\rm NN}} = 5 \sim 17.3A$ GeV) [11, 12] and also the CBM experiment at FAIR/GSI ($\sqrt{s_{\rm NN}} \leq 8.5A$ GeV) [13, 14, 15]. Many experimental observables have been also proposed to be the QCP signatures, such as dynamical fluctuations in K/π ratio [16], two experimental observables correlation [17], high order moment of transverse momentum [18], *etc.*.

In the hydrodynamical description of relativistic heavy ion collisions, the expansion of the central fireball should be regarded as isentropic for the negligible entropy production in the latter evolution, which can be represented as entropy density s to baryon density n_b ratio (s/n_b) to be constant [19]. A trajectory with $s/n_b = constant$ for a given colliding system on the QCD phase diagram is called isentropic trajectory. Recently, the critical singular properties of QCP have been implemented in equation of state (EOS) for hydrodynamical description of HICs [19, 20] by Asakawa, *et al.*. They pointed out that when the isentropic trajectory passes through the vicinity of the QCP, it may be deformed-the so-called "QCP focusing effect" [19]. They also argued that the QCP focusing effect may result in an observable anomaly in the β_t dependence of $\bar{p}/p$ ratio [21], which can be employed as a robust signature of the QCP. However, whether the focusing effect can effectively result in an observable anomaly in the β_t dependence of $\bar{p}/p$ ratio has not been worked out yet; neither has the corresponding mechanism. In this letter, we will formulate the QCP focusing effect on the β_t dependence of $\bar{p}/p$ ratio and apply the UrQMD and THERMINATOR model to calculate the dependence patterns for three gedanken focused isentropic trajectories with different focusing degrees on the QCD phase diagram.

The UrQMD model [22] used here is based on the quark, di-quark, string and hadronic degrees of freedom and relativistic Boltzmann transport dynamics. It includes 50 different baryon species(nucleon, hyperon and their resonances up to 2.11 GeV) and 25 different meson species. It is usually used to describe the freeze-out and breakup of the fireball produced in relativistic heavy-ion collisions into hadrons. The model has successfully been applied to reproduce the experimental results from SIS/GSI to SPS/CERN energies [23]. The THERMINATOR model [24] is a Monte-Carlo event generator designed for studying of particle production in relativistic heavy ion collisions from SPS to LHC energies. It implements thermal models of particle production with single freeze out. The input parameters are those thermodynamical parameters at freeze out, such as temperature T, baryon chemical potential μ_B, *etc.*.

*Corresponding author: xfluo@lbl.gov

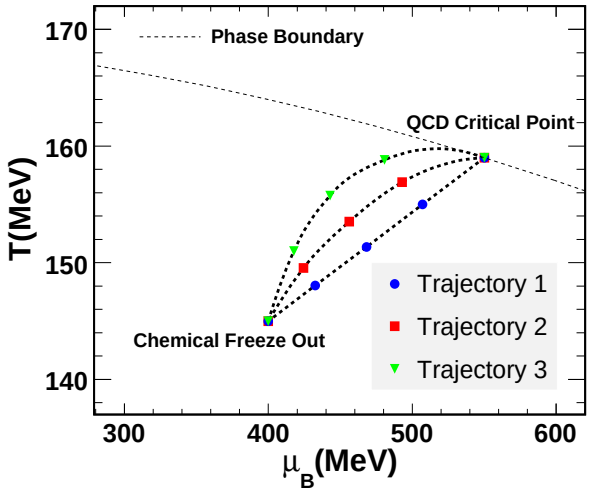

FIG. 1: Three gedanken isentropic trajectories on the QCD phase diagram with different focusing degrees. All trajectories meet at the same QCD critical point (550,159) MeV and chemical freeze out point (400,145) MeV on the phase diagram.

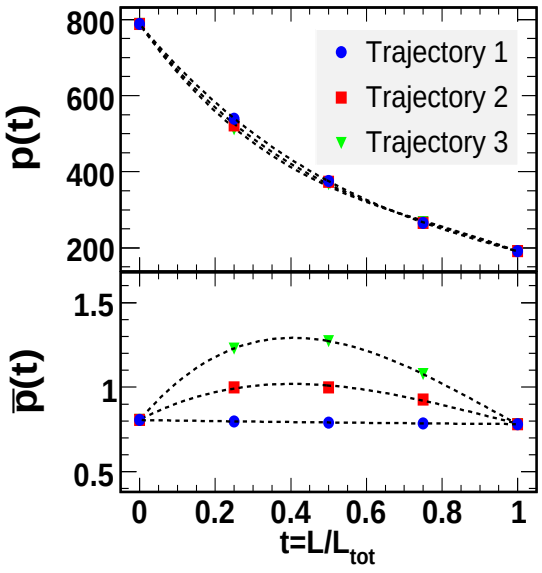

FIG. 2: The normalized time evolution of the proton(upper panel) and antiproton (lower panel) numbers along the three gedanken isentropic trajectories.

II. FORMULATION OF THE QCD CRITICAL POINT FOCUSING EFFECT

To quantitatively describe the QCP focusing effect, three gedanken isentropic trajectories with different focusing degrees, passing through the common QCP and chemical freeze out point are constructed on the (μ_B, T) plane and respectively labeled as Trajectory 1, 2 and 3 in Fig.1. The location of the QCP (μ_c, T_c)=(550,149) MeV chosen here is the same as the Ref. [21], and the chemical freeze out point (μ_{ch}, T_{ch})=(440,145) MeV is the statistical model fit result to the data of Pb+Pb 40A GeV fixed target reactions at SPS/CERN [25]. Besides the start and end points, three other (μ_B, T) points are also sampled for every trajectory. As the actual evolution time scale of the isentropic trajectory on the QCD phase diagram is unknown, the normalized time is used and defined by the normalized path length, $t = L/L_{tot}$. For each isentropic trajectory, the L represents the path length along the trajectory from the considered point to the QCP and L_{tot} is the length along the trajectory from the chemical freeze out point to QCP. The colliding system is evolving from the QCP along the isentropic trajectory to the chemical freeze out point and assumed to be thermodynamical equilibrium. Then, the μ_B and T of every sampling point are used as the input thermodynamical parameters for THERMINATOR model to calculate the corresponding antiproton and proton numbers along the corresponding isentropic trajectory on QCD phase diagram.

The normalized time dependence of the antiproton and proton numbers at the sampled points for the three gedanken isentropic trajectories are respectively shown in Fig.2, in which the dash lines are the corresponding 3rd-order polynomial fitting results. It is found in Fig.2 that QCP focusing effect results in a sharp decrease of proton number and a non-monotonous increase of antiproton number along the focused isentropic trajectory. We can also see large discrepancy among the antiproton numbers of the three trajectories, whereas there is little discrepancy for the proton number. This means the antiproton is much more sensitive to the focusing degree than proton. In Fig. 3, the time evolution of $\bar{p}/p$ ratio along the three gedanken isentropic trajectories and the corresponding 3rd-order polynomial fitting dash lines are shown. The antiproton to proton number ratio $(\bar{p}/p)$ increases monotonously from QCP $(t = 0)$ to chemical freeze out point $(t = 1)$, which can be simply explained as the decreasing value of μ_B/T along each focused isentropic trajectory [21].

Although we have obtained three gedanken focused isentropic trajectories, the quantitative description of the QCP focusing effect on β_t dependence of $\bar{p}/p$ ratio and also the corresponding mechanism are still ambiguous. In qualitative analysis, particles with large β_t would be emitted earlier from the fireball created in HICs, since the mean free path generally grows with increasing hadron momentum and becomes comparable with the fireball size [21]. In Fig. 4, the transverse velocity (β_t) dependences of the average emission time ($< t_{emission} >$) for antiproton and proton in Pb+Pb 40 AGeV fixed target reactions are calculated by UrQMD. It is implied that the antiproton and proton, which are dynamically emitted from the fireball, would show strong $\beta_t - t$ anti-correlation during the cooling down of the colliding system. The general $\beta_t - t$ anti-correlation pattern cannot

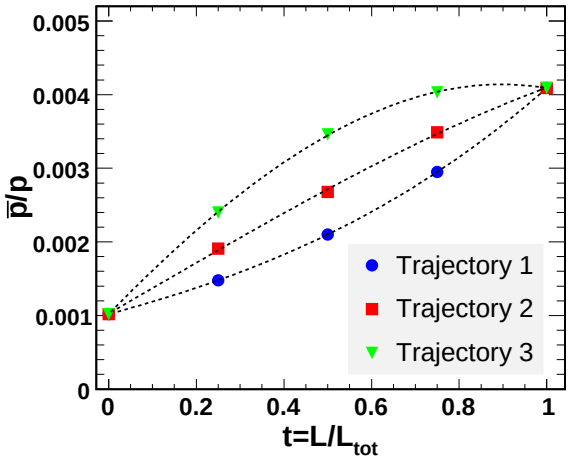

FIG. 3: The normalized time evolution of the antiproton to proton ratio for three gedanken isentropic trajectories.

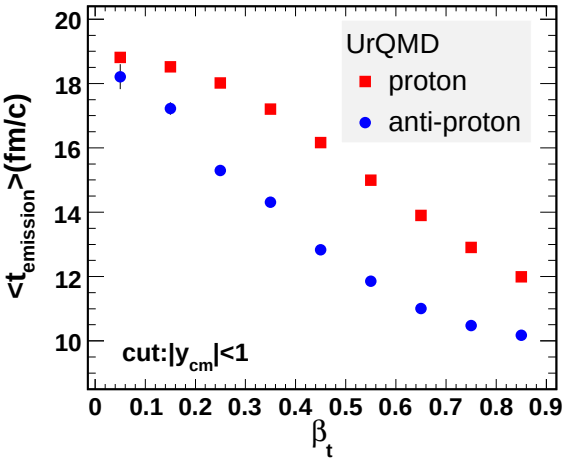

FIG. 4: The average emission time $< t_{emission} >$ dependence of the transverse velocity β_t calculated by UrQMD for Pb+Pb 40 AGeV fixed target reactions at mid-rapidity.

be reproduced by hydrodynamic inspired model for their particular particle freeze out mechanism. The significant increase of $\bar{p}/p$ ratio with the normalized time t shown in Fig. 3, together with the strong β_t-t anti-correlation indicates the experimental observable, β_t dependence of $\bar{p}/p$ ratio, should be enhanced in the lower β_t region and suppressed in the higher β_t region [21].

The formulation of the QCP focusing effect on β_t dependence of $\bar{p}/p$ ratio is based on two simple assumptions: one is that the numbers of antiproton and proton evolve independently along the isentropic trajectories and the other is that the numbers of antiproton and proton emitted at time t are proportional to their corresponding total number ($\bar{p}(t)$, $p(t)$). The two assumptions can be formulated as:

$$\bar{p}(t) = k_1 \times \int N_{\bar{p}}(\beta_t, t)\mathrm{d}\beta_t \tag{1}$$

$$p(t) = k_2 \times \int N_p(\beta_t, t)\mathrm{d}\beta_t \tag{2}$$

,where the $N_{\bar{p}}(\beta_t, t)$ and $N_p(\beta_t, t)$ are the two-dimensional $\beta_t - t$ distributions of the antiproton and proton, respectively. The two $\beta_t - t$ distributions indicate antiproton and proton are emitted from the colliding system with a finite probability for certain emission time t and transverse velocity β_t. The k_1 and k_2 are the two unknown constant coefficients. In addition to equ.(1) and (2), we also have the boundary condition:

$$\bar{p}(1) = k_1 \times \int N_{\bar{p}}(\beta_t, 1)\mathrm{d}\beta_t = \int_0^1 \int N_{\bar{p}}(\beta_t, t)\mathrm{d}\beta_t\mathrm{d}t \tag{3}$$

$$p(1) = k_2 \times \int N_p(\beta_t, 1)\mathrm{d}\beta_t = \int_0^1 \int N_p(\beta_t, t)\mathrm{d}\beta_t\mathrm{d}t \tag{4}$$

, which means the numbers of antiproton and proton at chemical freeze out point ($t = 1$) are equal to their corresponding sum of emitted numbers along the isentropic trajectory.

The two constants k_1 and k_2 can be determined by performing integral over the normalized time t on both sides of equ. (1) and (2), respectively as:

$$k_1 = \frac{\int_0^1 \bar{p}(t)\mathrm{d}t}{\int_0^1 \int N_{\bar{p}}(\beta_t, t)\mathrm{d}\beta_t\mathrm{d}t} = \frac{\int_0^1 \bar{p}(t)\mathrm{d}t}{\bar{p}(1)} \tag{5}$$

$$k_2 = \frac{\int_0^1 p(t)\mathrm{d}t}{\int_0^1 \int N_p(\beta_t, t)\mathrm{d}\beta_t\mathrm{d}t} = \frac{\int_0^1 p(t)\mathrm{d}t}{p(1)} \tag{6}$$

We introduce $D_{\bar{p}}(t)$ and $D_p(t)$ as the numbers of antiproton and proton emitted at time t along the isentropic trajectory, respectively. Then, with equ. (1), (2), (5) and (6), we have:

$$D_{\bar{p}}(t) = \int N_{\bar{p}}(\beta_t, t)\mathrm{d}\beta_t = \frac{\bar{p}(t)}{k_1} = \frac{\bar{p}(t)}{\int_0^1 \bar{p}(t)\mathrm{d}t} \times \bar{p}(1) \tag{7}$$

$$D_p(t) = \int N_p(\beta_t, t)\mathrm{d}\beta_t = \frac{p(t)}{k_2} = \frac{p(t)}{\int_0^1 p(t)\mathrm{d}t} \times p(1) \tag{8}$$

It is found that the $D_{\bar{p}}(t)$ and $D_p(t)$ are only determined by the normalized time t dependence of antiproton and proton numbers along the isentropic trajectory, respectively, which are calculated by THERMINATOR model in Fig. 2.

The experimental observable, β_t dependence of $\bar{p}/p$ ratio, can be calculated as:

$$\frac{\bar{p}(\beta_t)}{p(\beta_t)} = \frac{\int_0^1 N_{\bar{p}}(\beta_t, t)\mathrm{d}t}{\int_0^1 N_p(\beta_t, t)\mathrm{d}t} \tag{9}$$

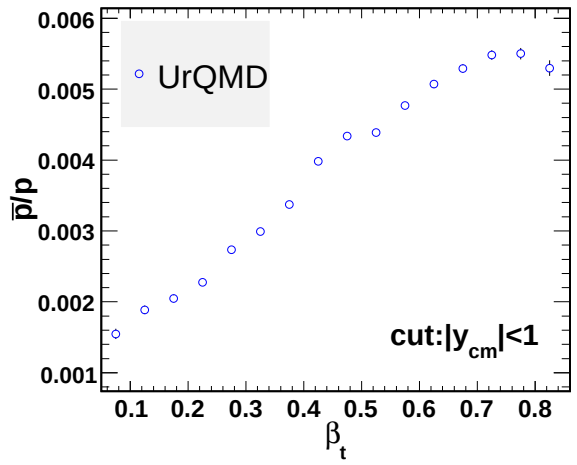

FIG. 5: β_t dependence of $\bar{p}/p$ ratio calculated by UrQMD for Pb+Pb 40 AGeV fixed target reactions at mid-rapidity.

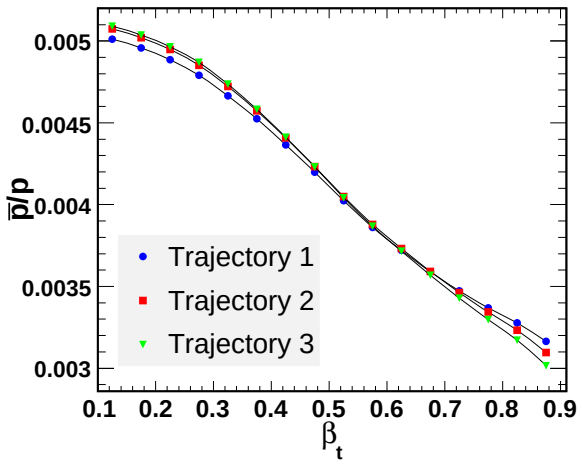

FIG. 6: β_t dependence of $\bar{p}/p$ ratio for three gedanken isentropic trajectories. The solid lines are used to guide eyes.

, which depends strongly on the $\beta_t - t$ distributions of antiproton and proton. Although, the two $\beta_t - t$ distributions are not exactly known, the anti-correlation between β_t and t is well known.

To quantitatively analyze and set the benchmark for the β_t dependence of $\bar{p}/p$ ratio with the QCP focusing effect, we extract the $\beta_t - t$ distributions of antiproton ($N^U_{\bar{p}}(\beta_t, t)$) and proton ($N^U_p(\beta_t, t)$) from the Pb+Pb 40 AGeV fixed target reactions implemented by UrQMD. The emission time t here has been normalized. With the two $\beta_t - t$ distributions, the corresponding β_t dependence of $\bar{p}/p$ ratio is calculated by equ.(9) and shown in Fig.5. As QGP phase transition and QCP have not been implemented in UrQMD model, the monotonous increase pattern with β_t up to 0.7 in Fig. 5 is thought to be normal and without suffering from QCP focusing effect.

In order to obtain the anomalous β_t dependence of $\bar{p}/p$ ratio resulted from the QCP focusing effects, we modify the $\beta_t - t$ distributions of antiproton ($N^U_{\bar{p}}(\beta_t, t)$) and proton ($N^U_p(\beta_t, t)$), which has been calculated by UrQMD model. The t distributions in the $N^U_{\bar{p}}(\beta_t, t)$ and $N^U_p(\beta_t, t)$ are replaced by the distributions $D_{\bar{p}}(t)$ and $D_p(t)$ derived from equ.(7) and (8), respectively. For the three gedanken focused isentropic trajectories in Fig. 1, the resulted $\beta_t - t$ distributions for antiproton and proton, which have been introduced in QCP focusing effect, can be calculated as:

$$N^{QCP}_{\bar{p}}(\beta_t, t) = \frac{N^U_{\bar{p}}(\beta_t, t)}{\int N^U_{\bar{p}}(\beta_t, t)\mathrm{d}\beta_t} \times D_{\bar{p}}(t) \qquad (10)$$

$$N^{QCP}_{p}(\beta_t, t) = \frac{N^U_{p}(\beta_t, t)}{\int N^U_{p}(\beta_t, t)\mathrm{d}\beta_t} \times D_{p}(t) \qquad (11)$$

Consequently, the QCP focusing effect has been implemented in the $\beta_t - t$ distributions for both antiproton and proton through the equ.(10) and (11), respectively. Thus, the β_t dependence of $\bar{p}/p$ ratio with QCP focusing effect can be also calculated by equ.(9) with the modified $\beta_t - t$ distributions ($N^{QCP}_{\bar{p}}(\beta_t, t)$, $N^{QCP}_{p}(\beta_t, t)$). The results for the three focused gedanken isentropic trajectories on the QCD phase diagram are illustrated in Fig. 6. Comparing the results of UrQMD calculation in Fig. 5 and the results with QCP focusing effect in Fig. 6, we find that they demonstrate completely opposite dependence patterns, which indicates the QCP focusing effect could actually result in an observable anomaly in the β_t dependence of $\bar{p}/p$ ratio. In Fig.6, it is also noticed that the higher focused degree of isentropic trajectory leads to the steeper β_t dependence of $\bar{p}/p$ ratio. Obviously, the anomalous β_t dependence of $\bar{p}/p$ ratio can be employed as a sensitive QCP signature.

III. SUMMARY AND DISCUSSION

We have formulated the QCP focusing effect on β_t dependence of $\bar{p}/p$ ratio with some reasonable assumptions. The quantitative calculations for the three gedanken focused isentropic trajectories have been made with UrQMD and THERMINATOR models. In fact, the real $\beta_t - t$ correlation pattern for antiproton and proton of a colliding system in HICs cannot be measured experimentally, which directly determines the β_t dependence of $\bar{p}/p$ ratio. Therefore, the UrQMD model is used to provide $\beta_t - t$ correlation pattern and the THERMINATOR model is applied to calculate the normalized time dependence of the antiproton and proton numbers along the isentropic trajectories. Then, the anomalous β_t dependence of $\bar{p}/p$ ratios have been obtained for three gedanken focused isentropic trajectories, which means the QCP focusing effect can efficiently result in an observable anomaly in the β_t dependence of $\bar{p}/p$ ratio. We

argue that when the isentropic trajectory of the colliding system on the QCD phase diagram is passing through the vicinity of the QCP and deformed by QCP focusing effect, an observable anomaly in β_t dependence of $\bar{p}/p$ ratio, enhanced in low β_t and suppressed in high β_t region, will be observed. This anomaly may also be reflected in the p_T spectra of antiproton and/or proton. The existing antiproton p_T spectrum for Pb+Pb 40 AGeV fixed target collisions measured by NA49 collaboration at SPS/CERN exhibits a steeper exponential slope [21, 26]. Finally, we propose that it may be helpful to extract the anomalous structures from the p_T spectrum of antiproton and/or proton by performing inverse Laplace transform on the spectrum [27]. The excitation function of structure variable, which should be predefined, can be useful to search for the QCP.

IV. ACKNOWLEDGEMENT

This work is supported by the National Natural Science Foundation of China (10835005, 10675111, 10775131).

[1] P. Braun-Munzinger, J. Wambach, arXiv:0801.4256.
[2] N. Xu *et al*, Nucl. Phys. **A 751** (2005) 109-126 .
[3] J. Adams *et al*, Nucl. Phys. **A 757** (2005) 102-183.
[4] K. Adcox *et al*, Nucl. Phys. **A 757** (2005) 184-283.
[5] F. Karsch, arXiv:hep-lat/0601013.
[6] Z. Fodor, S. D. Katz, JHEP **0203** (2002) 014.
[7] M. Stephanov, Acta Phys. Polon. **B 35** (2004) 2939-2962; arXiv:hep-lat/0701002.
[8] P. Sorensen, arXiv:nucl-ex/0701028.
[9] ROYA. Lacey *et al*, Phys. Rev. Lett. **98** (2007) 092301.
[10] GSF Stephans, J. Phys. G: Nucl. Part. Phys. **35** (2008) 044050.
[11] A. Laszlo *et al.* (NA61 Collaboration), arXiv:0709.1867.
[12] M. Gazdzicki, arXiv:nucl-ex/0512034.
[13] J. M. Heuser (CBM Collaboration), J. Phys. G: Nucl. Part. Phys. **35** (2008) 4.
[14] P. Senger, Acta Physica Hungarica a-Heavy Ion Physics **22** (2005) 363.
[15] S. Chattopadhyay (CBM Collaboration), J. Phys. G: Nucl. Part. Phys. **35** (2008) 104027.
[16] M.A. Stephanov, K. Rajagopal, and E.V. Shuryak, Phys. Rev. **D 60** (1999) 114028.
[17] X. F. Luo *et al.*, Phys. Rev. **C 78**(R) (2008) 031901.
[18] J. X. Du *et al.*, arXiv:0810.1989.
[19] C. Nonaka and M. Asakawa, Phys. Rev. **C 71** (2005) 044904.
[20] C. Nonaka, M. Asakawa and S. A. Bass, J. Phys. G: Nucl. Part. Phys. **35** (2008) 104099.
[21] M. Asakawa, *et al.*, Phys. Rev. Lett. **101** (2008) 122302.
[22] S.A. Bass *et al.*, Prog. Part. Nucl. Phys. **41** (1998) 255.
[23] L. A. Winckelmann *et al.*, arXiv:nucl-th/9610033.
[24] A. Kisiel *et al*, Computer Physics Communications **174** (2006) 669.
[25] P. Braun-Munzinger, K. Redlich and J. Stachel, arXiv:nucl-th/0304013.
[26] C. Alt *et al.* (NA49 Collaboration), Phys. Rev. **C 73** (2006) 044910.
[27] E. Schnedermann, Z. Phys. **C 64** (1994) 85-90.